Biochemical and Biophysical Research Communications 445 (2014) 126–131

Contents lists available at ScienceDirect

Biochemical and Biophysical Research Communications

journal homepage: www.elsevier.com/locate/ybbrc

Loss of AMP-activated protein kinase in X-linked adrenoleukodystrophy patient-derived fibroblasts and lymphocytes

Jaspreet Singh *, Shailendra Giri

Department of Neurology, Henry Ford Health System, Detroit, MI 48202, United States

ARTICLE INFO

Article history:
Received 21 January 2014
Available online 1 February 2014

Keywords:
AMPKα1
X-ALD
Ubiquitin
Inflammation
OCR
ECAR

ABSTRACT

X-Adrenoleukodystrophy (X-ALD) is a peroxisomal disorder characterized by accumulation of very-long-chain (VLC) fatty acids, which induces inflammatory disease and alterations in cellular redox, both of which are reported to play a role in the pathogenesis of the severe form of the disease (childhood cerebral ALD). While the mutation defect in ABCD1 gene is common to all forms of X-ALD it fails to account for the spectrum of phenotypic variability seen in X-ALD patients, strongly suggesting a role for as yet unidentified modifier gene(s). Here we report, for the first time, loss of AMP-activated protein kinase alpha1 (AMPKα1) in patient-derived fibroblasts and lymphocytes of the severe cerebral form of X-ALD (ALD), and not in the milder adrenomyeloneuropathy (AMN) form. Decrease in AMPK was observed at both protein and mRNA levels. AMPK loss in ALD patient-derived fibroblasts was associated with increased ubiquitination. Using the Seahorse Bioscience XF^{e}96 Flux Analyzer for measuring the mitochondrial oxygen consumption and extracellular acidification rate we show that ALD patient-derived fibroblasts have a significantly lower "metabolic state" than AMN fibroblasts. Unstimulated ALD patient-derived lymphocytes had significantly higher proinflammatory gene expression. Selective AMPK loss represents a novel physiopathogenic factor in X-ALD disease mechanism. Strategies aimed at upregulating/recovering AMPK levels might have beneficial therapeutic effects in X-ALD.

1. Introduction

Childhood cerebral X-linked adrenoleukodystrophy (X-ALD) is a rapidly progressive inflammatory demyelinating disease with severe cognitive and neurologic disability leading to a vegetative state within 2–5 years of clinical onset of symptoms and death [1]. A milder form of X-ALD is named as adrenomyeloneuropathy (AMN) and characterized by a non-inflammatory distal axonopathy mostly in spinal cord [1]. Both childhood cerebral ALD (ALD) and the milder AMN phenotypes are caused by mutations in ABCD1 gene encoding peroxisomal membrane ABC transporter adrenoleukodystrophy protein (ALDP). Virtually nothing is known regarding the mechanisms that lead to neuroinflammation in patients with ALD. Role of an as yet unidentified modifier gene is well accepted [1,2]. X-ALD males in the same family may express different phenotypes, thus it is clear that mutations of the *ABCD1* gene alone does not account for the disease variability [1,2]. AMP-activated protein kinase (AMPK) plays an important role in controlling energy homeostasis and is envisioned as a promising target to treat metabolic disorders [3]. Disturbances in AMPK are implicated in neuroinflammatory diseases [4,5] including multiple sclerosis [6,7]. Our striking observation of loss of AMPKα1 in ALD patient-derived cells but not AMN and healthy controls suggests a novel role for AMPKα1 in the mechanism of neuroinflammation and disease progression in X-ALD.

AMPK is a serine/threonine kinase which is activated via allosteric regulation of increased AMP concentration and by the phosphorylation of α subunit (Thr172) [3]. One major role of AMPK signaling is to respond to metabolic requirements by inhibiting energy consuming pathways, e.g., synthesis of protein, fatty acids, and cholesterol and promotes ATP producing catabolic pathways including fatty acid oxidation [3]. Although traditionally regarded as the master energy regulator of the cell, recent extensive literature demonstrates that AMPK can also suppress the expression of inflammatory genes and attenuate inflammatory injury [5,6]. Genetic or pharmacological inhibition of AMPK is associated with increased inflammation *in vivo* and *in vitro* [4–10].

In this study, we report, for the first time, a differential loss of AMPK in human ALD patient-derived fibroblasts and lymphocytes. Further, we observed that AMPK was targeted for degradation through ubiquitination. Bioenergetic analysis utilizing Seahorse

* Corresponding author. Address: Department of Neurology, E&R Bld, Room#7092, Henry Ford Health System, Detroit, MI 48202, United States. Fax: +1 313 916 1318.
E-mail address: jsingh2@hfhs.org (J. Singh).

http://dx.doi.org/10.1016/j.bbrc.2014.01.126
0006-291X/

Bioscience Extracellular Flux Analyzer showed that loss of AMPK was also associated with "low metabolic" profile of ALD-patient derived fibroblasts. The relevance of AMPK loss in X-ALD has yet to be tested directly, but it likely represents an important role in disease mechanism that may be targeted for therapy.

2. Materials and methods

2.1. Reagents

Dulbecco's Modified Eagle's Medium (DMEM, 4.5 g/L) and RPMI-1640 was purchased from Invitrogen Life Technologies; fetal bovine serum (FBS) was purchased from BioAbChem Inc. (Ladson, SC) and Hanks' balanced salt solution (HBSS) was purchased from Gibco (Invitrogen, Carlsbad, CA). Antibodies were purchased from Cell Signaling Technology Inc. unless otherwise mentioned. ECL and nitrocellulose membranes were purchased from Amersham Biosciences.

2.2. Cell culture

All patient-derived cells were obtained from the NIGMS Human Genetic Cell Repository at the Coriell Institute for Medical Research (ccr.coriell.org).

2.2.1. Fibroblasts

Human skin fibroblasts (derived from normal control (CTL1; GM03348, CTL2; GM03377), ALD (ALD1; GM04934, ALD2; GM04904), and AMN (AMN1; GM07531, AMN2; GM17819) patients were cultured in DMEM containing 15% FBS and antibiotic/antimycotic.

2.2.2. Lymphocytes

Human lymphocytes derived from normal (control; GM03798), female carrier (HTZ, GM04674), and ALD (ALD1; GM04673, ALD2; GM13496) patients were cultured in RPMI1640 containing 10% FBS and antibiotic/antimycotic.

2.3. Immunoblot analysis

0.7×10^6 cells/10 mL fibroblasts and 0.5×10^6 cells/10 mL lymphocytes from control, AMN and ALD were cultured for 16 h and processed for immunoblot analysis as described previously [11].

2.4. RNA extraction and cDNA synthesis

RNA was extracted using RNAeasy mini kit (Qiagen) per the manufacturer's protocol, single-stranded cDNA was synthesized from two microgram of total RNA using iScript cDNA synthesis kit (BioRad).

2.5. Real-time PCR

Real time PCR was conducted using CFX96 Real Time PCR Detection System (Bio-Rad). Single-stranded cDNA was synthesized from total RNA as described [11]. The primer sets were purchased from SA Bioscience (Qiagen). iTaq™ Univer SYBR Green Supermix was from Bio-Rad. Thermal cycling conditions were as follows: activation of DNA polymerase at 95 °C for 3 min, followed by 40 cycles of amplification at 95 °C for 30 s and 60 °C for 30 s. The normalized expression (^^Ct) of target gene with respect to ribosomal protein L27 expression was analyzed using CFX Manager Software.

2.6. Co-immunoprecipitation (Co-IP) and immunoblot analysis

Cells were lysed in lysis buffer (20 mM Tris–HCl (pH 7.4), 150 mM NaCl, 1 mM EDTA, 1 mM EGTA, 1% Trion X-100, 2.5 mM sodium pyrophosphate, 1 mM β-glycerol phosphate, 1 mM sodium orthovandate, 2 μg/ml leupeptin and 1 mM PMSF). Co-IP was performed using protein A/G beads (Santa Cruz Biotechnology) in the presence of antibodies against ubiquitin (Santa Cruz Biotechnology) and AMPKα1. The Co-IP products were then subjected to SDS–PAGE and immunoblot analysis.

2.7. Measurement of mitochondrial oxygen consumption and extracellular flux

To monitor the consumption of oxygen and extracellular acidification in intact adherent fibroblasts, Seahorse Bioscience XF^e96 Extracellular Flux Analyzer was used (Seahorse Bioscience, North Billerica, MA, USA). For these experiments, fibroblasts were seeded to 3×10^4 cells/well in 12 wells (for each cell line) of XF^e 96-well cell culture microplate (Seahorse Bioscience) in 200 μL of DMEM and incubated overnight (14–16 h) at 37 °C in 5% CO_2 atmosphere. After replacing the growth medium with 175 μL of bicarbonate-free DMEM pre-warmed at 37 °C cells were preincubated at 37 °C for 1 h for degassing before starting the assay procedure. Oxygen consumption rate (OCR) and extracellular acidification rate (ECAR) was measured using mix/wait/measure times of 3/3/3 min. After baseline measurements of OCR and ECAR, OCR was measured after sequentially adding to each well 25 μL of oligomycin (1 μM), carbonyl cyanide-ptrifluoromethoxyphenylhydrazone (FCCP) (0.25 μM), and Rotenone/antimycin A (1 μM) and ECAR by glucose (10 μM), oligomycin (2 μM) and 2-deoxyglucose (100 μM) to the indicated final concentrations using the included ports on the XF^e96 cartridges. Further analysis of these experiments was performed as described [12]. Metabolic profile of the individual cell lines was generated by plotting OCR against ECAR.

2.8. Determination of ATP levels

2×10^4 cells/well were seeded in 96 well cell culture plate in complete medium. After 16–18 h cells, were lysed in 20 μl lysis buffer and 10 μl of lysate was used to measure ATP levels using ATP determination Kit (Molecular Probes, Invitrogen). 1 μl each of the remaining lysate was used for protein measurement.

2.9. Statistical analysis

Using the Student Newman–Keuls test and ANOVA, p values were determined for the respective experiments using GraphPad software (GraphPad Software Inc. San Diego, CA).

3. Results and discussion

3.1. AMPK subunit levels are reduced in ALD patient-derived fibroblasts and lymphocytes

The molecular events associated with the transition from a relatively benign metabolic disease to a fatal neuroinflammatory disease in X-ALD are not well understood at present. Interestingly, AMPK downregulation is associated with increased proinflammatory response [6,7,13]. To examine the status of AMPK in different phenotypes of X-ALD, we measured AMPKα1 phosphorylation in control, AMN and ALD human patient-derived fibroblasts and lymphocytes (Fig. 1). Fibroblasts (7×10^4 cells/mL) and lymphocytes (5×10^4 cells/mL) were cultured in complete medium and harvested after 16–18 h for mRNA and immunoblot analysis. The

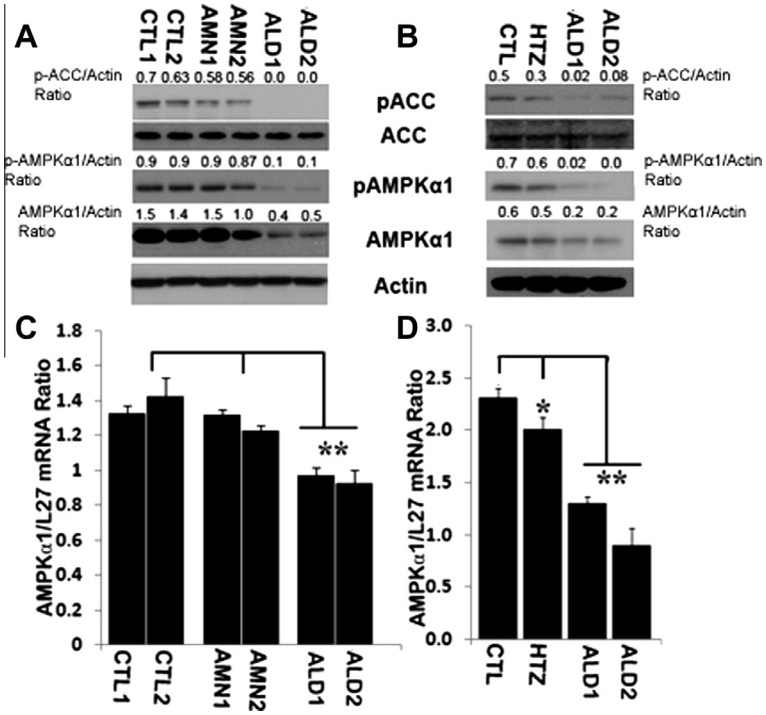

Fig. 1. AMPKα1 protein and mRNA levels are reduced in ALD patient-derived fibroblasts and lymphocytes. Human control (CTL1, CTL2), AMN (AMN1, AMN2) and ALD (ALD1, ALD2) patient-derived skin fibroblasts (A and C) and lymphocytes (B and D) were cultured as described in Section 2. After 16–18 h Cells were harvested for immunoblot (A and B) and quantitative real-time RT-PCR (C and D). Protein levels of p-AMPKα1, AMPKα1, p-ACC and ACC were analyzed by immunoblot analysis in whole cell lysate. Densitometry values were normalized to β-actin. RNA was isolated using RNAeasy mini kit (Qiagen) and cDNA prepared from 2 μg total RNA per sample. 20 ng cDNA per sample was amplified by qRT-PCR. Gene expression was normalized to L27 expression. Data are represented as mean ± SD of three different experiments. $^{*}P < 0.05$; $^{**}P < 0.01$. HTZ, heterozygote female carrier lymphocytes.

activation of AMPK was evaluated by detection of phosphorylation of AMPKα1 (p-AMPKα1) at Thr-172 [6,10]. As shown in Fig. 1, fibroblasts (Fig. 1A) and lymphocytes (Fig. 1B) from healthy control subjects showed strong p-AMPKα1 and total AMPKα1 levels. Expectedly, strong phosphorylation of acyl-CoA carboxylase (ACC), a bonafide substrate of AMPK and an indicator of AMPK activity [10], was observed in fibroblasts (Fig. 1A) and lymphocytes (Fig. 1B) of control healthy subjects. Phosphorylation inactivates ACC1, leading to inhibition of *de novo* fatty acid and cholesterol synthesis [6]. ACC is a rate-determining enzyme for the synthesis of malonyl–CoA, both a critical substrate for fatty acid biosynthesis and a potent inhibitor of fatty acid oxidation [6]. The phosphorylation status of ACC and AMPKα1 levels were largely unchanged in AMN patient-derived fibroblasts compare to healthy control, however, they were slightly reduced in female carrier (HTZ)-patient-derived lymphocytes (Fig. 1B). Strikingly, the phosphorylation of both ACC and AMPKα1 and also total AMPKα1 levels were significantly decreased in ALD patient-derived cells (Fig. 1A and B). Quantitative RT-PCR (qRT-PCR) revealed that the reduction of total protein levels was mirrored by significantly lower ($P < 0.01$) mRNA levels of AMPKα1 in ALD patient-derived fibroblasts (Fig. 1C). In lymphocytes, AMPKα1 were significantly reduced ($P < 0.05$) in female heterozygote carriers and further decreased significantly ($P < 0.01$) in ALD patient-derived lymphocytes (Fig. 1D). While the decrease in AMPKα1 protein was associated with increased ubiquitination (discussed below) the reduced mRNA expression may be a result of changes in turnover or decrease in promoter activity [14].

AMPK is a trimer containing α, β, γ subunits, all of which are essential for its activity [15]. The expressions of the three different subunits should be regulated tightly to keep their levels in balance to form a functional AMPK complex [15]. This may explain their differential regulation [7,15] that was also evident in our system (Suppl. Fig. S1). We further analyzed the expression of remaining AMPK subunits ($\alpha 2$, $\beta 1$, $\beta 2$, $\gamma 1$, $\gamma 2$, and $\gamma 3$) in control healthy, AMN and ALD patient-derived fibroblasts and lymphocytes (Suppl. Fig. S1). AMPKα2 was decreased in ALD patient-derived fibroblasts at both protein and mRNA levels (Suppl. Fig. S1A). AMPKα2 protein was not detected in any of the patient-derived lymphocytes (Suppl. Fig. S1B) supporting the previous observations that AMPKα2 is not expressed in lymphocytes or immune cells in general [6,7]. Further, total protein expressions of $\beta 1/2$ and $-\gamma 1$ subunits were also significantly decreased in ALD patient-derived fibroblasts (Suppl. Fig. S1A) and lymphocytes (Suppl. Fig. S1B). qRT-PCR analysis using subunit-specific primers revealed that the variation in protein levels of AMPK subunits were mimicked by changes in mRNA expressions (Suppl. Fig. S1C and D). Our data, for the first time, documents an overall decrease in AMPK levels in the severe form (ALD) of X-ALD. Because no clear physiological function have been attributed to each AMPK trimer despite availability of knock out and transgenic mice models [16], the functional implications of altered subunit levels and expression in X-ALD observed in the present study await further investigations. The observations, however, could be particularly relevant to X-ALD pathology considering the fact that AMPK protein expression and activity are conclusively related to fatty acid oxidation, mitochondrial biogenesis function [17] and negatively regulate the inflammatory response [4–9,13,18]. Our observation of an association between downregulation of AMPKα1 in a particular phenotype of X-ALD (Fig. 1) furthers demonstrates that AMPK subunits express independently of each other and provides evidence on the complexity of genetic alterations, in addition to the common ABCD1 defect, in different phenotypes of X-ALD.

3.2. AMPKα1 is associated with ubiquitin degradation pathway in ALD

While we understand the basic regulation of AMPK activity by upstream kinases, recent studies have introduced the concept that

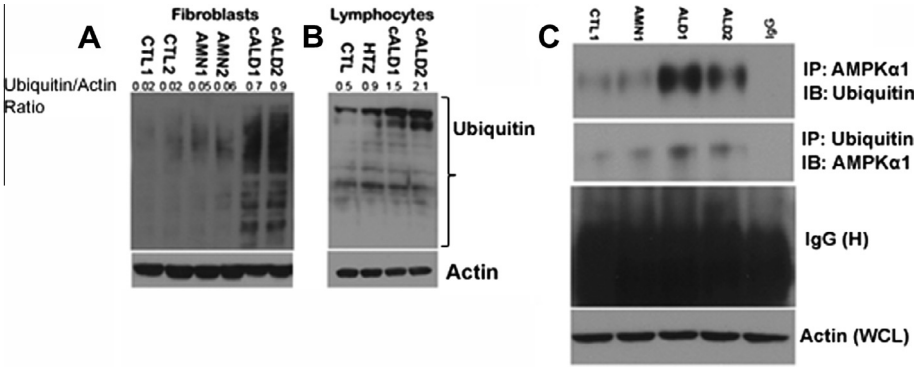

Fig. 2. AMPKα1 is ubiquitinated in ALD patient-derived fibroblasts and lymphocytes. Human control (CTL1, CTL2), AMN (AMN1, AMN2) and ALD (ALD1, ALD2) patient-derived skin fibroblasts (A and C) and lymphocytes (B) were cultured as described in Section 2. Ubiquitin levels in fibroblasts (A) and lymphocytes (B) were analyzed in 50 μg of whole cell lysates. (C) 500 μg of whole cell lysate per sample was used for immunoprecipitation (IP) using ubiquitin and AMPKα1 antibodies. The pull-down was resuspended in 50 μl of gel loading buffer and used for detection of AMPKα1 and ubiquitin, respectively by western blot. 30 μl of starting whole cell lysate (WCL) used for IP was blotted for β-actin as loading control.

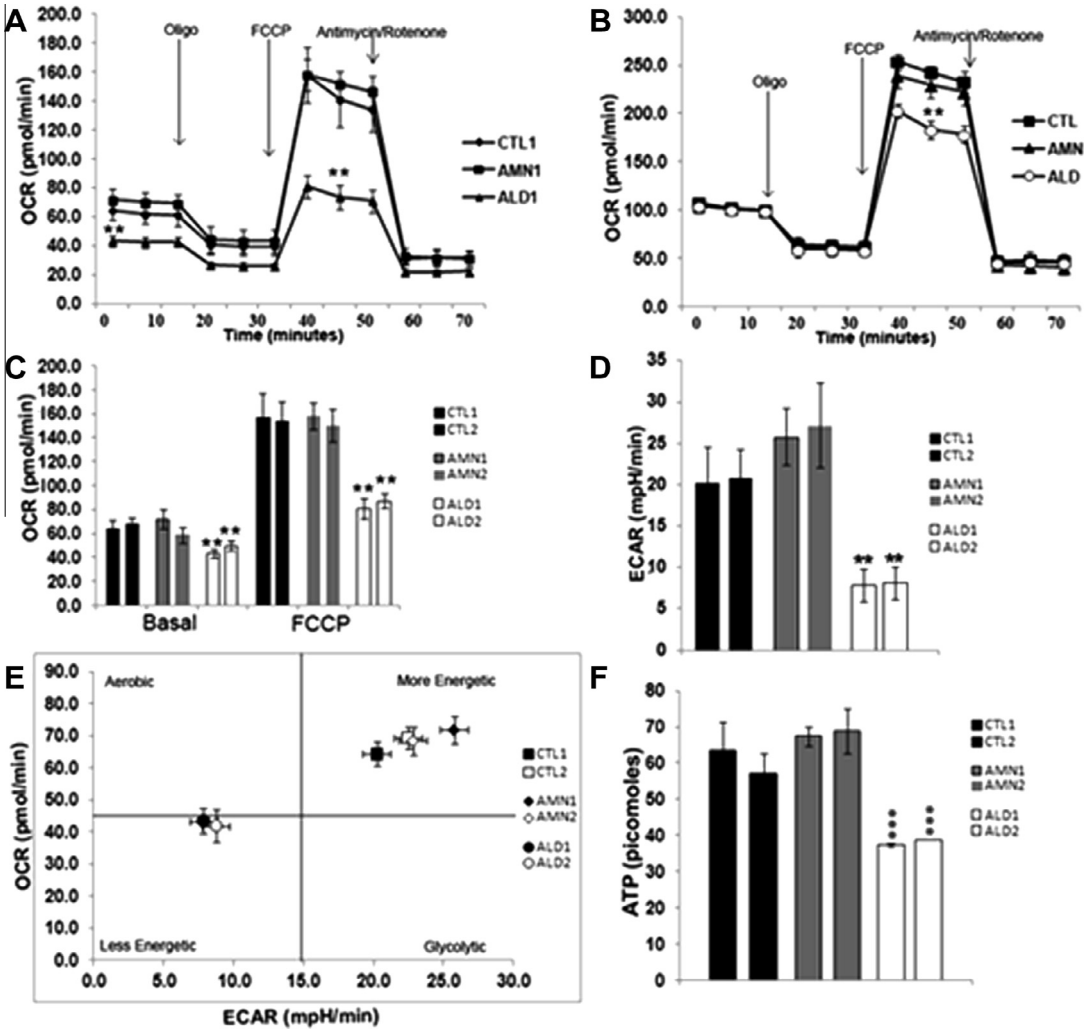

Fig. 3. Baseline energetics and intracellular ATP levels. Fibroblasts cells were seeded to 3×10^4 cells/well in XF96 V3-PS cell culture microplate (Seahorse Bioscience). After 16–18 h, cells were changed to assay media. (A) Representative basal oxygen consumption rate (OCR) profile of control (CTL), AMN and ALD patient-derived fibroblasts. (B) Representative basal oxygen consumption rate (OCR) profile of control (CTL), AMN and ALD patient-derived fibroblasts. (C) Both basal and FCCP-coupled OCR was significantly reduced in ALD patient-derived fibroblasts (D) ECAR was measured in parallel with respiration. Each data point represents mean ± SD ($n = 12$), and results are representative of 4 independent experiments. mpH, milli-pH units. (E) OCR and ECAR are plotted against each other for the duration of the experiment to generate a "metabolic profile". Decreased OCR (C) and decreased ECAR (D) result in a overall decreased OCR/ECAR ratio for ALD patient-derived fibroblasts resulting in their localization to "low energy" quadrant. (F) Intracellular ATP level was measured as described in Section 2. ATP level is expressed as mean ± SD ($n = 12$) and results are representative of 3 independent experiments. $^{**}P < 0.01$; $^{***}P < 0.001$.

AMPK is regulated by other post-translational modifications, specifically ubiquitination [19]. Ubiquitination of proteins is also increased in X-ALD fibroblasts and Abcd1-ko mice [20]. However, difference in ubiquitin levels (if any) between AMN and ALD patient-derived cells are not known. Interestingly, we found a significant difference in ubiquitin levels between AMN and ALD patient-derived fibroblasts (Fig. 2A) and lymphocytes (Fig. 2B). Higher level of ubiquitinated proteins was observed in ALD fibroblasts and lymphocytes compared to AMN (Fig. 2A and B). Immunoprecipitation by ubiquitin (or AMPKα1) antibody and subsequent immunoblotting for AMPKα1 (or ubiqutin) in patient-derived fibroblasts showed that AMPKα1 was associated with ubiquitin in both AMN and ALD patient-derived cells but the association was much stronger in ALD (Fig. 2C).

3.3. Mitochondrial maximal respiratory capacity is significantly reduced in ALD compared to AMN patient-derived fibroblasts

Mitochondrial dysfunction was recently reported in X-ALD [21–23]. Given the central role of AMPK in regulating mitochondrial content and function [17], the premise that AMPK downregulation might play an impending role in mitochondrial dysfunction in X-ALD is highly expected. We used a Seahorse XF^{e}96 Analyzer (Seahorse Bioscience, Billerica, MA) to assess the metabolic profile of control healthy, AMN and ALD patient-derived fibroblasts (Fig. 3A). Measurement of oxygen consumption rate (OCR), a measure of oxidative phosphorylation, and extracellular acidification rate (ECAR), a measure of glycolysis, gives an overall metabolic status of the cell [12]. In line with a recent report [23], control healthy and AMN patient-derived cells had comparable basal and FCCP-uncoupled OCR (Fig. 3A–C). However, the differences, if any, between the AMN and ALD phenotypes were not addressed previously [23]. FCCP-uncoupled OCR also represents the maximum respiratory capacity (MRC) of mitochondria and hence is a measure of mitochondrial electron transport chain integrity [24]. We document, for the first time, a significantly reduced basal and FCCP-uncoupled OCR (MRC) in ALD compared to AMN patient-derived fibroblasts (Fig. 3A–C). Importantly, FCCP-uncoupled MRC was significantly reduced in ALD patient-derived fibroblasts even when the basal OCR levels were normalized between control, AMN and ALD patient-derived fibroblasts (Fig. 3B). In addition to OCR, ECAR levels were also significantly reduced in ALD patient-derived fibroblasts compared to AMN and control (Fig. 3D). Ratio of OCR to ECAR indicates the "metabolic profile or state" of a cell [25]. We, therefore, plotted OCR against ECAR to compare the "metabolic state" of control, AMN and ALD patient-derived fibroblasts (Fig. 3E). No such evaluation is available for for AMN and ALD cells. Due to higher OCR and ECAR levels, the ECAR/OCR ratio of control and AMN patient-derived fibroblasts was localized in the "more energetic" (and hence metabolically active) quadrant (Fig. 3E). On the other hand, ECAR/OCR ratio of ALD patient-derived fibroblasts localized to "less energetic" (and hence metabolically less active) quadrant (Fig. 3E). ALD patient-derived fibroblasts were less energetic due to both reduced OCR and ECAR (Fig. 3C and D). Since AMPK and mitochondrial OXPHOS activity regulates ATP levels [5,17,26,27]. Mice with genetic deletion(s) of AMPK subunits have reduced mitochondrial content [27]. Further, these mice have reduced mitochondrial respiration and basal ATP levels [26]. Therefore, we next measured the ATP content in control healthy, AMN and ALD patient-derived fibroblasts (Fig. 3F). Consequent to comparable AMPKα1 levels and OCR activities, ATP levels were well-maintained between control healthy and AMN patient-derived fibroblasts (Fig. 3F). On the other hand, ATP levels were significantly reduced in ALD patient-derived fibroblasts compared to AMN (Fig. 3F). This raises the possibility that loss of AMPKα1 in ALD patient-derived fibroblasts may be responsible for the lower bioenergetic profile (Fig. 3A–E) and hence reduced ATP levels (Fig. 3F).

3.4. Inflammatory cytokine gene expression is increased in unstimulated ALD patient-derived lymphocytes

Although, traditionally associated with cellular metabolism, the relationship between decreased AMPK levels and the inflammatory phenotype of X-ALD (ALD) observed in our study is in keeping with previous reports where decrease in AMPK activity and expression have been shown to result in increased inflammatory response [4,7,8]. AMPKα1 is crucial for anti-inflammatory skewing of immune cells [5,6,8,9] and is involved in inhibiting lipid-induced macrophage inflammation [18]. Indeed, AMPK knockout animal models consistently demonstrate reduced mitochondrial biogenesis/function [16] and increased pro-inflammatory skewing [5,8,9,18]. Unstimulated ALD patient-derived lymphocytes produce proinflammatory cytokines under serum-free condition [28]. We examined the expression of inducible nitric oxide synthase (iNOS), interleukin-6 (IL-6) and tumor necrosis factor-α (TNF-α) under normal culture conditions where we had observed AMPKα1-loss (media with FBS). Expression of iNOS and IL-6 mRNA was increased in ALD patient-derived unstimulated lymphocytes (Fig. 4). There was no change in expression of TNF-α (data not shown). Such associations raise the possibility that AMPKα1 may regulate the inflammatory response observed in ALD phenotype. The observed loss of AMPKα1 in ALD-patient-derived cells though novel was not totally unexpected as inflammatory stimuli and a fatty acid rich-diet decreased the expression and activity of AMPKα1 and triggered TNF-α expression in mouse adipose tissue and macrophages [29]. Also, circulating free fatty acids (FFAs) in obesity activate TLR4-NFKB-inflammation pathway [30] and activation of same pathway by endotoxin results in loss of AMPK activity in activated macrophages [6]. Furthermore, psychosine-mediated downregulation of AMPK generates neuroinflammatory response in astrocytes and leads to oligodendroglial death in an *in vitro* model of Krabbe disease, a neurometabolic disorder [10]. Our results provide the first mechanistic underpinnings of transition of a benign metabolic phenotype (AMN) to fatal neuroinflammatory disease (ALD) and raise the intriguing possibility that diminished

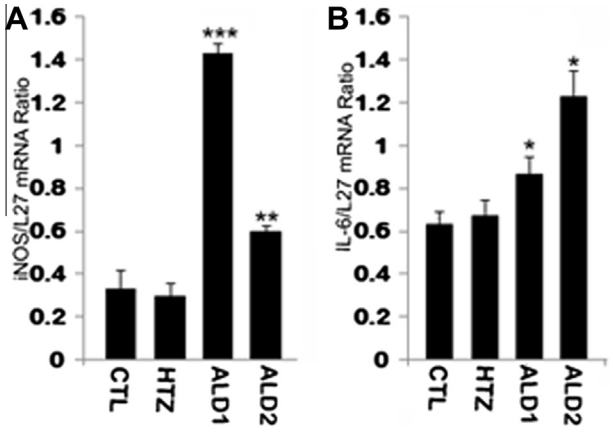

Fig. 4. iNOS and IL-6 gene expression is increased in unstimulated ALD patient-derived lymphocytes. Control (CTL), heterozygote carrier (HTZ) and ALD (ALD1, ALD2) patient-derived lymphocytes were culture (0.5×10^6/10 mL) in RPMI-1640 with 10% FBS and antibiotic in 25 cm^2 flasks. Cells were pelleted after 16–18 h and RNA isolated using RNAeasy mini kit (Qiagen). 2 μg total RNA was reverse transcribed to cDNA and used at final concentration of 20 ng/rxn in SYBR Green qPCR reaction (CFX96, BIO RAD). iNOS and IL-6 gene expression were normalized to L27 expression. Data are represented as mean ± SD of three different experiments. $^*P < 0.05$; $^{**}P < 0.01$; $^{***}P < 0.001$.

AMPKα1 levels in ALD phenotype and increased inflammation could be causal factors for each other. If so, whether one of them is the initiating event in humans remains to be determined. In conclusion, reduced mitochondrial function and increased inflammatory response in ALD patient-derived fibroblasts suggests that down regulation of AMPKα1 is a physio-pathogenic factor that may act as the transition trigger from a metabolic to inflammatory disease in X-ALD. This provides an exciting target to interfere and possibly reverse the progression of disease in X-ALD.

Acknowledgment

This work was supported by Proposal Development Grant (A30916) of Henry Ford Health System to J.S.

Appendix A. Supplementary data

Supplementary data associated with this article can be found, in the online version, at http://dx.doi.org/10.1016/j.bbrc.2014.01.126.

References

[1] M. Engelen, S. Kemp, M. de Visser, B.M. van Geel, R.J. Wanders, P. Aubourg, B.T. Poll-The, X-linked adrenoleukodystrophy (X-ALD): clinical presentation and guidelines for diagnosis, follow-up and management, Orphanet J. Rare Dis. 7 (2012) 51.
[2] I. Singh, A. Pujol, Pathomechanisms underlying X-adrenoleukodystrophy: a three-hit hypothesis, Brain Pathol. 20 (2010) 838–844.
[3] C. Canto, J. Auwerx, AMP-activated protein kinase and its downstream transcriptional pathways, Cell. Mol. Life Sci. 67 (2010) 3407–3423.
[4] M.S. Gauthier, E.L. O'Brien, S. Bigornia, M. Mott, J.M. Cacicedo, X.J. Xu, N. Gokce, C. Apovian, N. Ruderman, Decreased AMP-activated protein kinase activity is associated with increased inflammation in visceral adipose tissue and with whole-body insulin resistance in morbidly obese humans, Biochem. Biophys. Res. Commun. 404 (2011) 382–387.
[5] L.A. O'Neill, D.G. Hardie, Metabolism of inflammation limited by AMPK and pseudo-starvation, Nature 493 (2013) 346–355.
[6] N. Nath, M. Khan, M.K. Paintlia, I. Singh, M.N. Hoda, S. Giri, Metformin attenuated the autoimmune disease of the central nervous system in animal models of multiple sclerosis, J. Immunol. 182 (2009) 8005–8014.
[7] N. Nath, M. Khan, R. Rattan, A. Mangalam, R.S. Makkar, C. de Meester, L. Bertrand, I. Singh, Y. Chen, B. Viollet, S. Giri, Loss of AMPK exacerbates experimental autoimmune encephalomyelitis disease severity, Biochem. Biophys. Res. Commun. 386 (2009) 16–20.
[8] K.C. Carroll, B. Viollet, J. Suttles, AMPKalpha1 deficiency amplifies proinflammatory myeloid APC activity and CD40 signaling, J. Leukoc. Biol. 94 (2013) 1113–1121.
[9] R. Mounier, M. Theret, L. Arnold, S. Cuvellier, L. Bultot, O. Goransson, N. Sanz, A. Ferry, K. Sakamoto, M. Foretz, B. Viollet, B. Chazaud, AMPKalpha1 regulates macrophage skewing at the time of resolution of inflammation during skeletal muscle regeneration, Cell Metab. 18 (2013) 251–264.
[10] S. Giri, M. Khan, N. Nath, I. Singh, A.K. Singh, The role of AMPK in psychosine mediated effects on oligodendrocytes and astrocytes: implication for Krabbe disease, J. Neurochem. 105 (2008) 1820–1833.
[11] J. Singh, M. Khan, I. Singh, Silencing of Abcd1 and Abcd2 genes sensitizes astrocytes for inflammation: implication for X-adrenoleukodystrophy, J. Lipid Res. 50 (2009) 135–147.
[12] R.A. Schuh, P. Clerc, H. Hwang, Z. Mehrabian, K. Bittman, H. Chen, B.M. Polster, Adaptation of microplate-based respirometry for hippocampal slices and analysis of respiratory capacity, J. Neurosci. Res. 89 (2011) 1979–1988.
[13] N. Nath, S. Giri, R. Prasad, M.L. Salem, A.K. Singh, I. Singh, 5-aminoimidazole-4-carboxamide ribonucleoside: a novel immunomodulator with therapeutic efficacy in experimental autoimmune encephalomyelitis, J. Immunol. 175 (2005) 566–574.
[14] C.W. Lee, L.L. Wong, E.Y. Tse, H.F. Liu, V.Y. Leong, J.M. Lee, D.G. Hardie, I.O. Ng, Y.P. Ching, AMPK promotes p53 acetylation via phosphorylation and inactivation of SIRT1 in liver cancer cells, Cancer Res. 72 (2012) 4394–4404.
[15] D.G. Hardie, AMP-activated protein kinase: an energy sensor that regulates all aspects of cell function, Genes Dev. 25 (2011) 1895–1908.
[16] B. Viollet, Y. Athea, R. Mounier, B. Guigas, E. Zarrinpashneh, S. Horman, L. Lantier, S. Hebrard, J. Devin-Leclerc, C. Beauloye, M. Foretz, F. Andreelli, R. Ventura-Clapier, L. Bertrand, AMPK: lessons from transgenic and knockout animals, Front Biosci. (Landmark Ed.) 14 (2009) 19–44.
[17] H.M. O'Neill, G.P. Holloway, G.R. Steinberg, AMPK regulation of fatty acid metabolism and mitochondrial biogenesis: implications for obesity, Mol. Cell. Endocrinol. 366 (2013) 135–151.
[18] S. Galic, M.D. Fullerton, J.D. Schertzer, S. Sikkema, K. Marcinko, C.R. Walkley, D. Izon, J. Honeyman, Z.P. Chen, B.J. van Denderen, B.E. Kemp, G.R. Steinberg, Hematopoietic AMPK beta1 reduces mouse adipose tissue macrophage inflammation and insulin resistance in obesity, J. Clin. Investig. 121 (2011) 4903–4915.
[19] M. Zungu, J.C. Schisler, M.F. Essop, C. McCudden, C. Patterson, M.S. Willis, Regulation of AMPK by the ubiquitin proteasome system, Am. J. Pathol. 178 (2011) 4–11.
[20] N. Launay, M. Ruiz, S. Fourcade, A. Schluter, C. Guilera, I. Ferrer, E. Knecht, A. Pujol, Oxidative stress regulates the ubiquitin–proteasome system and immunoproteasome functioning in a mouse model of X-adrenoleukodystrophy, Brain 136 (2013) 891–904.
[21] J. Singh, M. Khan, A. Pujol, M. Baarine, I. Singh, Histone deacetylase inhibitor upregulates peroxisomal fatty acid oxidation and inhibits apoptotic cell death in abcd1-deficient glial cells, PLoS ONE 8 (2013) e70712.
[22] J. Singh, M. Khan, I. Singh, Caffeic acid phenethyl ester induces adrenoleukodystrophy (Abcd2) gene in human X-ALD fibroblasts and inhibits the proinflammatory response in Abcd1/2 silenced mouse primary astrocytes, Biochim. Biophys. Acta 2013 (1831) 747–758.
[23] J. Lopez-Erauskin, J. Galino, M. Ruiz, J.M. Cuezva, I. Fabregat, D. Cacabelos, J. Boada, J. Martinez, I. Ferrer, R. Pamplona, F. Villarroya, M. Portero-Otin, S. Fourcade, A. Pujol, Impaired mitochondrial oxidative phosphorylation in the peroxisomal disease X-linked adrenoleukodystrophy, Hum. Mol. Genet. 22 (2013) 3296–3305.
[24] C.C. Beeson, G.C. Beeson, R.G. Schnellmann, A high-throughput respirometric assay for mitochondrial biogenesis and toxicity, Anal. Biochem. 404 (2010) 75–81.
[25] B.P. Dranka, J. Zielonka, A.G. Kanthasamy, B. Kalyanaraman, Alterations in bioenergetic function induced by Parkinson's disease mimetic compounds: lack of correlation with superoxide generation, J. Neurochem. 122 (2012) 941–951.
[26] B. Guigas, L. Bertrand, N. Taleux, M. Foretz, N. Wiernsperger, D. Vertommen, F. Andreelli, B. Viollet, L. Hue, 5-Aminoimidazole-4-carboxamide-1-beta-D-ribofuranoside and metformin inhibit hepatic glucose phosphorylation by an AMP-activated protein kinase-independent effect on glucokinase translocation, Diabetes 55 (2006) 865–874.
[27] B. Guigas, N. Taleux, M. Foretz, D. Detaille, F. Andreelli, B. Viollet, L. Hue, AMP-activated protein kinase-independent inhibition of hepatic mitochondrial oxidative phosphorylation by AICA riboside, Biochem. J. 404 (2007) 499–507.
[28] T. Uto, M.A. Contreras, A.G. Gilg, I. Singh, Oxidative imbalance in nonstimulated X-adrenoleukodystrophy-derived lymphoblasts, Dev. Neurosci. 30 (2008) 410–418.
[29] Z. Yang, B.B. Kahn, H. Shi, B.Z. Xue, Macrophage alpha1 AMP-activated protein kinase (alpha1AMPK) antagonizes fatty acid-induced inflammation through SIRT1, J. Biol. Chem. 285 (2010) 19051–19059.
[30] H. Shi, M.V. Kokoeva, K. Inouye, I. Tzameli, H. Yin, J.S. Flier, TLR4 links innate immunity and fatty acid-induced insulin resistance, J. Clin. Investig. 116 (2006) 3015–3025.